Geophysical Studies of the Fly Ranch Northeast and Gerlach Northeast KGRA's, Nevada, 1980

Submitted to the Conservation Division by the

KGRA Geophysical Evaluation Project

Office of Geochemistry and Geophysics

U.S. Geological Survey

Index

Location and Geology

The Gerlach Northeast and Fly Ranch Northeast KGRA's are approximately 16 and 29 kilometers northeast of Gerlach in northwestern Nevada (see figure 1). Both KGRA's lie on the northwestern edge of the Black Rock Desert and east of the Granite Range. They lie on and adjacent to a bedrock ridge known as Steamboat ridge which is a horst block trending NNE separating the Black Rock Desert graben on the east from the Hualapai graben on the west.

Within the Gerlach Northeast KGRA, (fig. 2) the principal surficial deposits are modern playa deposits of the Black Rock Desert. Exposed in the western quarter are quaternary colluvium and alluvium and Permo-Triassic metavolcanics which comprise the Steamboat ridge (Grose and Sperandio, 1978). The fault along which the Black Rock Desert graben developed is inferred to cut across the KGRA in a northeasterly direction close to the contact between alluvial and playa deposits. A branch of this fault is inferred to run north-northwest towards Hualapi Flat within the KGRA.

There are no surface thermal manifestations within the K.G.R.A. Gerlach Hot Springs are about 8 miles to the southwest and Fly Ranch hot springs 8 miles to the northwest.

The Fly Ranch KGRA (fig. 3) is just south of the Calico Mountains which are comprised principally of Tertiary andesites with some silicic units cropping out in the southern end of the mountains. It is about 4 miles due east of the Fly Ranch hot springs.

The surficial deposits in the KGRA are almost entirely quaternary deposits of alluvium, colluvium and some dune sands. A small patch of playa deposits is present in the southeast part of the KGRA formed over the downdropped part of a half-graben. In the western part of the KGRA are two small outcrops of the Permo-Triassic metavolcanics which comprise the Steamboat Ridge. There also are no known surface thermal manifestations in this area either.

The main Black Rock Desert graben fault is inferred to run just at the southeast corner of the KGRA striking to the northeast (Keller and Grose, 1978). In addition two parallel faults are inferred which divide the KGRA into about thirds. Known faulting along which the Hualapi graben formed is present along the western edge of the KGRA.

Extensive geological and geophysical studies of the region are given in Keller and Grose (1978). These studies will not be summarized but will be referred to when appropriate.

Geophysical Data

Gravity data for the area is given by Crewdson in Keller and Grose (1978) along with microearthquake, reflection seismic, resistivity and electromagnetic data of several varieties. Aeromagnetic data is available from a published U.S.G.S. regional aeromagnetic survey.

As part of the KGRA evaluation detailed gravity surveys were made in the two KGRA's as well as audio-magnetotelluric surveys and E-field ratio telluric traverses. At the time the surveys were run data from Keller and Grose (1978) were not available. The data presented here however supplement that of Keller and Grose.

Details of the KGRA's will be discussed on an individual basis.

Aeromagnetic Survey

The aeromagnetic survey (fig. 4; USGS, 1972) was flown with flight lines approximately three kilometers apart and at 2.75 kilometers elevation above sea level. The data are contoured at a 20 gamma interval and thus, only large scale anomalies are defined. In this region of Nevada, the magnetic field is complex with most of the magnetic relief produced by the abundant intrusive and extrusive rocks of varying ages. The magnetic anomalies here reflect variations in topographic relief below the flight elevation, structure, lithology and remanent magnetization direction. The lacustrine sediments would be expected to be non-magnetic. Because of the map scale and anomaly wavelengths both the Gerlach Northeast and Fly Ranch Extension KGRA's will be discussed here.

In the surveyed area the thick lacustrine deposits of the Black Rock Desert and Hualapi Flat appear as magnetic lows as would be expected. Cutting across both KGRA's and trending generally north-northeast is a strong magnetic high which correlates with the Permo-Triassic metavolcanics of Steamboat Ridge. However a saddle in the magnetic high between the two KGRA's and inflection in the magnetic contours suggests that faulting may have offset these older units. This would be consistent with mapped north-northwest faulting in the area (Grose, 1978). If this association of the high magnetic values with the Permo-Triassic units is correct then the Fly Ranch NE KGRA would be underlain principally by these units with probably only a thin alluvial cover.

Tertiary silicic volcanics appear to be responsible for the small magnetic high in the south end of the Calico Mtns.

Gerlach Northeast KGRA

Gravity survey

A gravity survey consisting of forty-one stations was made in the area of the Gerlach Northeast KGRA. The data are presented as a simple Bouguer anomaly map (Fig. 5). No terrain corrections were made. Although terrain corrections are important in quantative interpretations, the simple Bouguer anomaly map is a satisfactory qualitative representative of the major gravity features particularly in this area where there is little topographic relief.

The gravity map shows the same general features as that of Crewdson (1978) except giving added detail. The principal features of the map are a north-northeast trending low in the eastern half of the KGRA with decreasing values to the south. The lowest values are toward the northwest side of the Black Rock Desert graben rather than in the center. These data with Crewdson's suggests that most of the down drop has been along the northeast trending fault running through the KGRA. The low reflects for the most part the low density lacustrine fill in the valley. The computed depth for the fill in the KGRA is 3000 ft (Crewdson, 1978).

A steep gravity gradient trends across the KGRA which approximately follows the inferred fault of Grose (1978). This probably reflects the principal fault along which the Black Rock Desert graben was downdropped. It is about 1.5 miles east of a mapped fault scarp at this location which bounds the Black Rock Desert.

An inflection in the steep gravity gradient occurs in the southwest part of the KGRA. This is inferred to be an inflection or branch in the fault at this location and correlated well with a fault branch inferred by Grose (1978) at about this position.

A poorly defined gravity high is seen in the northwest part of the surveyed area. Again looking at Crewdson's (1978) data it is clear that this reflects the higher density Permo-triassic metavolcanics which outcrop in Steamboat Ridge.

Audio-Magnetotelluric Survey

Thirteen AMT stations were occupied in the region of the Gerlach NE KGRA and three AMT maps were prepared. The first map is the average of orthogonal scalar apparent resistivities at 7.5 Hz (fig. 6). This is the deepest exploration frequency. The other two maps are apparent resistivities at 27 Hz for the north-south (fig. 7) and the east-west (fig. 8) of the telluric lines. The skin depth or approximate depth of penetration of the electromagnetic energy at 7.5 Hz is 185 meters in a 1 ohm-meter earth to 1850 meters in 100 ohm-meter material.

Within the KGRA a northeast trending low is seen which corresponds well with the gravity low. The resistivity rises slowly on the east and steep gradients are seen on the west. The higher resistivities on the west can be attributed to the Permo-Triassic rocks at or near the surface while the lower resistivities on the east are associated with the lacustrian lake deposits. The apparent resistivities under one ohm-meter can be considered unusual.

The maximum depth of exploration in these low resistivity playa deposits is about 100 meters yet there are significant differences in resistivity from the central low to the eastern edge of the KGRA. This may reflect leakage of saline thermal fluids along the northwest part of the playa to the near surface as the gravity data (Crewdson, 1978) shows the playa deposits to be much thicker than 100 meters in that part of the KGRA. An inflection in the steep resistivity gradient is also seen which corresponds well with inflection in the magnetic and gravity gradients in the same area.

The 27 Hz maps show the same trends as the 7.5 Hz maps. The differences between the two directions are what would be expected near a resistivity contrast, especially where the contrast trends north-south (same direction as one E-line).

<u>Telluric traverse survey</u>

One short E-field-ratio telluric traverse was made in the Gerlach KGRA (fig. 9). Because of the very low resistivities encountered on the playa, difficulty was encountered in obtaining sufficient natural signal strength so the survey was terminated due to lack of time.

The telluric survey results are shown in fig. 10. An abrupt drop in relative voltage of an order of magnitude (10x) occurs from dipole 0-1 to 2-3. This is equivalent to a resistivity change of two orders of magnitude (100x). The position and change in resistivity agree well with the AMT data but better define the electrical boundary. It should be noted that the electrical boundary is to the northwest of that indicated by the gravity data for the inferred fault location. This may imply that thermal waters are present or were present in the past and that alteration may have occurred within fractured portions of the Permo-Triassic rocks along the fault.

Fly Ranch Northeast KGRA

Gravity Survey

A gravity survey consisting of forty-four stations was made in the area of the Fly Ranch NE KGRA. The data are as before presented as a simple Bouguer anomaly map (fig. 11). As in the Gerlach NE KGRA there is little topographic relief so there are no large terrain corrections.

This map also shows the same general features as Crewdson (1978) but with more detail. The principal feature is the gravity high presumed associated with the Permo-Triassic units of Steamboat Ridge. No exposures are known in the area of the major high but a small outcrop of the Permo-Triassic metasediments is present in the south west corner of the KGRA near a second gravity high.

Steep gravity gradients beyond the east and west sides of the KGRA probably define the principal faults dividing the Steamboat Ridge from the Black Rock Desert basin on the east and the Hualapi basin on the west. On the west where the data defines the gradient trends better a northwest trending fault can be inferred. This appears to correlate with northwest trending faults mapped by Grose (1978) and Kumamoto (1978).

Audio-Magnetotelluric survey

Twelve AMT stations were occupied in the region of the Fly Ranch NE KGRA and three AMT maps were prepared as for the Gerlach NE KGRA.

The 7.5 Hz average map (fig. 12) shows the low resistivity playa sediments on the eastern border of the KGRA with a fairly steep gradient separating them from the higher resistivity of the Steamboat Ridge. The Ridge as it runs north either becomes more deeply buried beneath lower resistivity deposits, becomes altered or pinches out. An arcuate low resistivity zone is seen from the northeast corner to the southwest corner of the KGRA. It appears to be associated with the northwest margin of the buried Steamboat Ridge and probably represents faulting along that side of the Ridge. The lower resistivities could be due to thicker alluvium and/or thermal fluids rising along the fault. The higher resistivities further west are assumed to be due to the metasediments which crop out in the area.

The two 27 Hz maps, figs. 13 and 14 show similar patterns. The low station density and apparent complexity of the area preclude definitive statements regarding the differences in the two data sets.

Telluric traverse survey

Two E-field-ratio telluric traverses were run across the KGRA in parallel orientation running approximately southeast (fig. 15). This was approximately normal to the expected trends of the region.

On traverse one (fig. 16) a zone of high resistivity between stations 1 and 5 correlates with the metavolcanics of Steamboat Ridge in agreement with the other data sets. To the northwest a moderate low resistivity zone is seen which then gradually increases as the metasediments are approached. This probably is a small graben which would be nicely correlated with inferred faults shown on the geologic map, fig. 3. The data suggest that the graben formed on a series of faults rather than on each side due to the gentle sides on the profile.

Profile two (fig. 16) appears much more complex and reveals a great deal of faulting and or lithologic change along the profile. Because of the association with outcrop the high between stations 8 to 10 is believed to be the Permo-Triassic metavolcanics as is the high between 1 and 3 which is on strike of the Steamboat Ridge.

It is clear that there are some major changes in the region between the two traverses. This is suggested also in the AMT and gravity data as well. It also appears that the traverses did not run far enough east to define the principal electrical boundary between the KGRA and the playa.

Conclusions

The Gerlach NE and Fly Ranch NE KGRA's are characterized by moderately complex geophysical data which reflect the complex volcanic history of the region on top of more recent basin formation. There are no known thermal manifestations within the KGRA's.

The principle feature of the two areas is a ridge, Steamboat Ridge, only partly reflected in topography which trends northeast across the areas. This ridge is expressed in the geophysical data as a magnetic, gravity, and electrical resistivity high. These data suggest that the ridge is a horst block separating the Black Rock Desert basin from the much smaller Hualapi basin to the west and in which the Fly Ranch Hot Springs are located.

Within the Black Rock Desert, the location of hot springs is found to be controlled by faulting, often occurring at intersections or inflections of faults. Local seismic activity then provides the means (minor active faulting) to maintain the system open. Because of this the Gerlach NE appears to be the most favorable of the two. Kumamoto (1978) shows that the majority of earthquake epicenters occurs within or very close to the Gerlach NE KGRA providing clear evidence for a mechanism acting at the present time to keep the system open. Also the low resistivities may be indicative of the presence of thermal waters leaking up along the fault.

Also the slight discordance in the location of the gravity and electrical boundary along the principal fault may suggest thermal waters in the older metavolcanics.

The Fly Ranch NE KGRA does not appear promising; however, the arcuate low on the northwest side of the buried Steamboat may be a possible target. Additional information is needed to resolve some of the complexities of this KGRA.

References

Aeromagnetic map of parts of the Lovelock, Reno, and Millet 1° by 2° quadrangle, Nevada, by U.S. Geological Survey, scale 1:250,000, Open File Report 1972.

Crewdson, R. A., 1978, "A gravity survey of Hualapai Flat and the southern part of the Black Rock Desert, Nevada", Studies of a Geothermal System in Northwestern Nevada - Part 1, Colorado School of Mines Quarterly, vol. 73, no. 3.

Grose, L. T. and R. J. Sperandio, 1978, "Geologic Map of the Gerlach-Hualapai Flat Area", Studies of a Geothermal System in Northwestern Nevada - Part 1, Colorado School of Mines Quarterly, vol. 73, no. 3.

Keller, G. V., and L. T. Grose (eds.), 1978, Studies of a Geothermal System in Northwestern Nevada, Colorado School of Mines Quarterly, vol. 73, no. 3 and 4.

Kumamoto, L., 1978, "Microearthquake Survey in the Gerlach - Fly Ranch area of northwestern Nevada", Studies of a Geothermal System in Northwestern Nevada - Part 1, Colorado School of Mines Quarterly, vol. 73, no. 3.

List of Figures

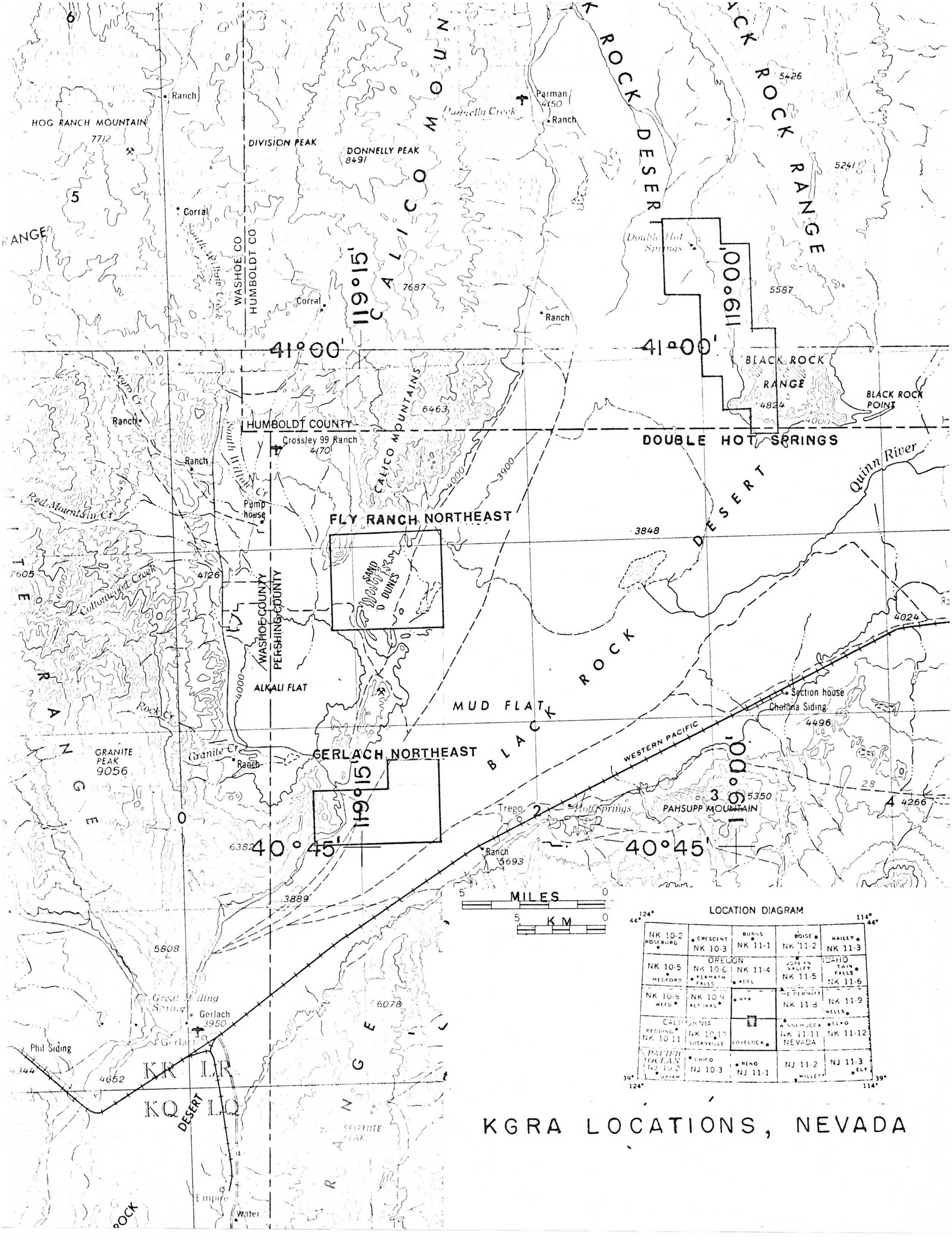

KGRA LOCATIONS, NEVADA

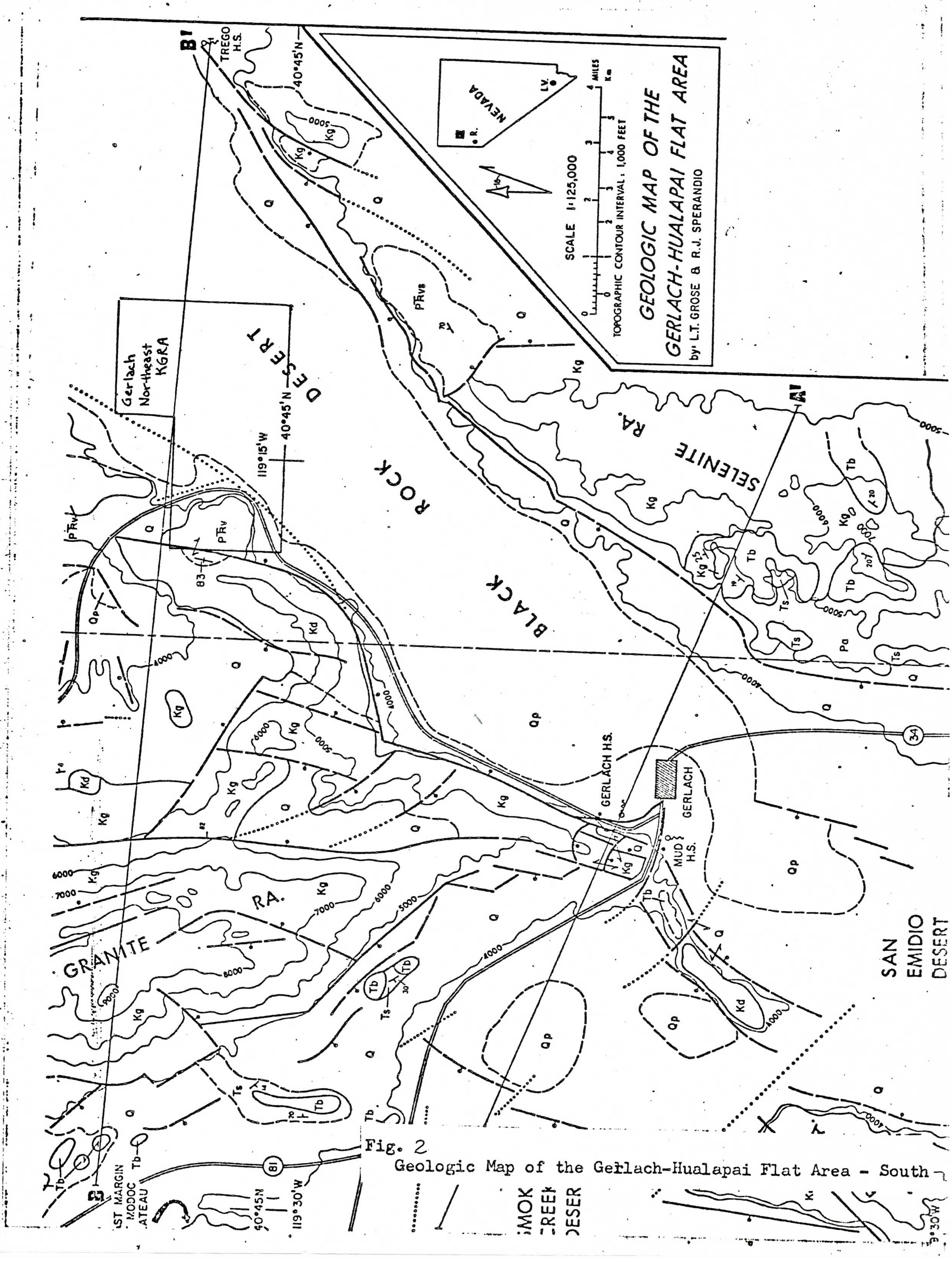

Fig. 2
Geologic Map of the Gerlach-Hualapai Flat Area - South

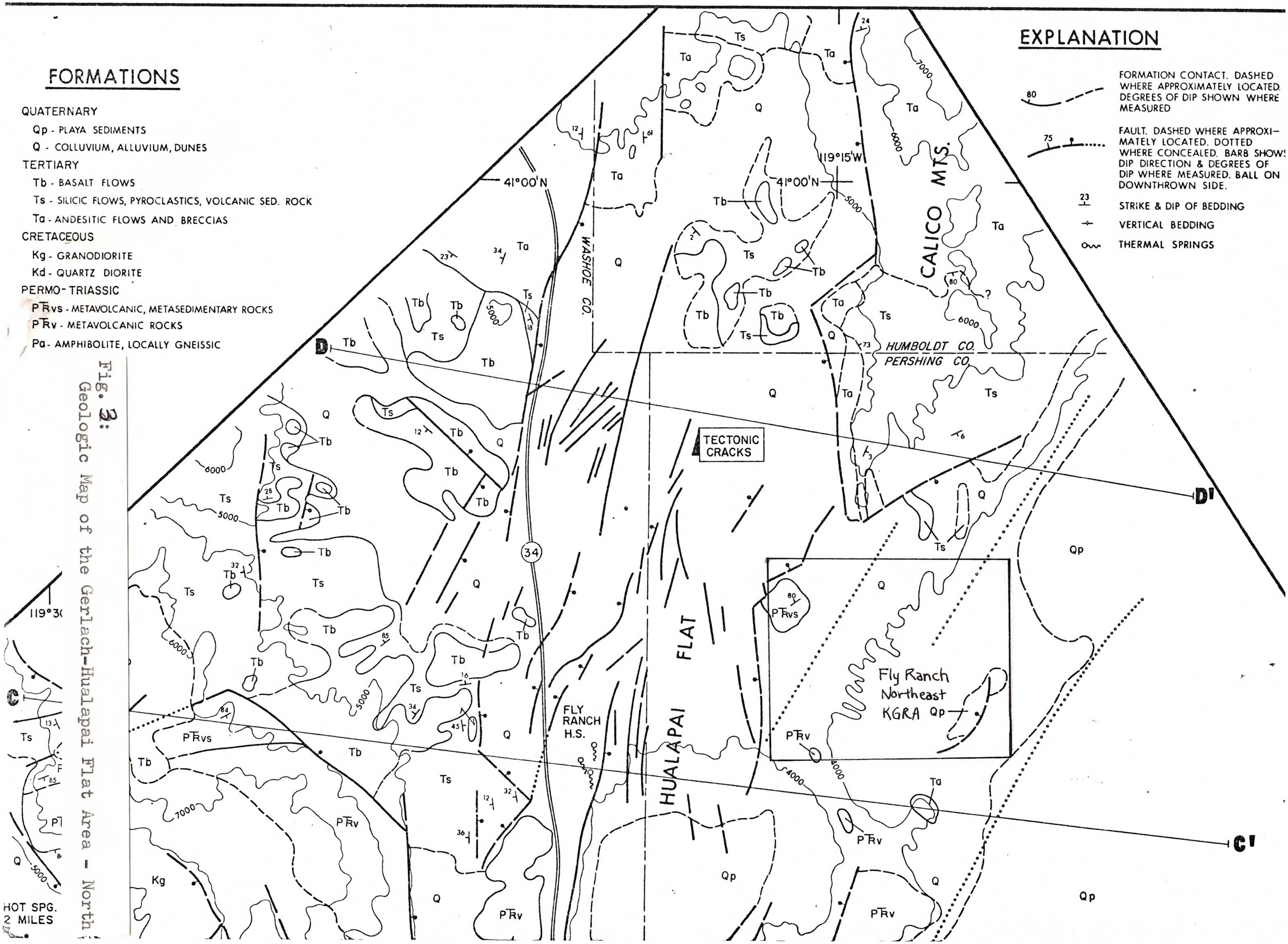

Fig. 3: Geologic Map of the Gerlach-Hualapai Flat Area - North

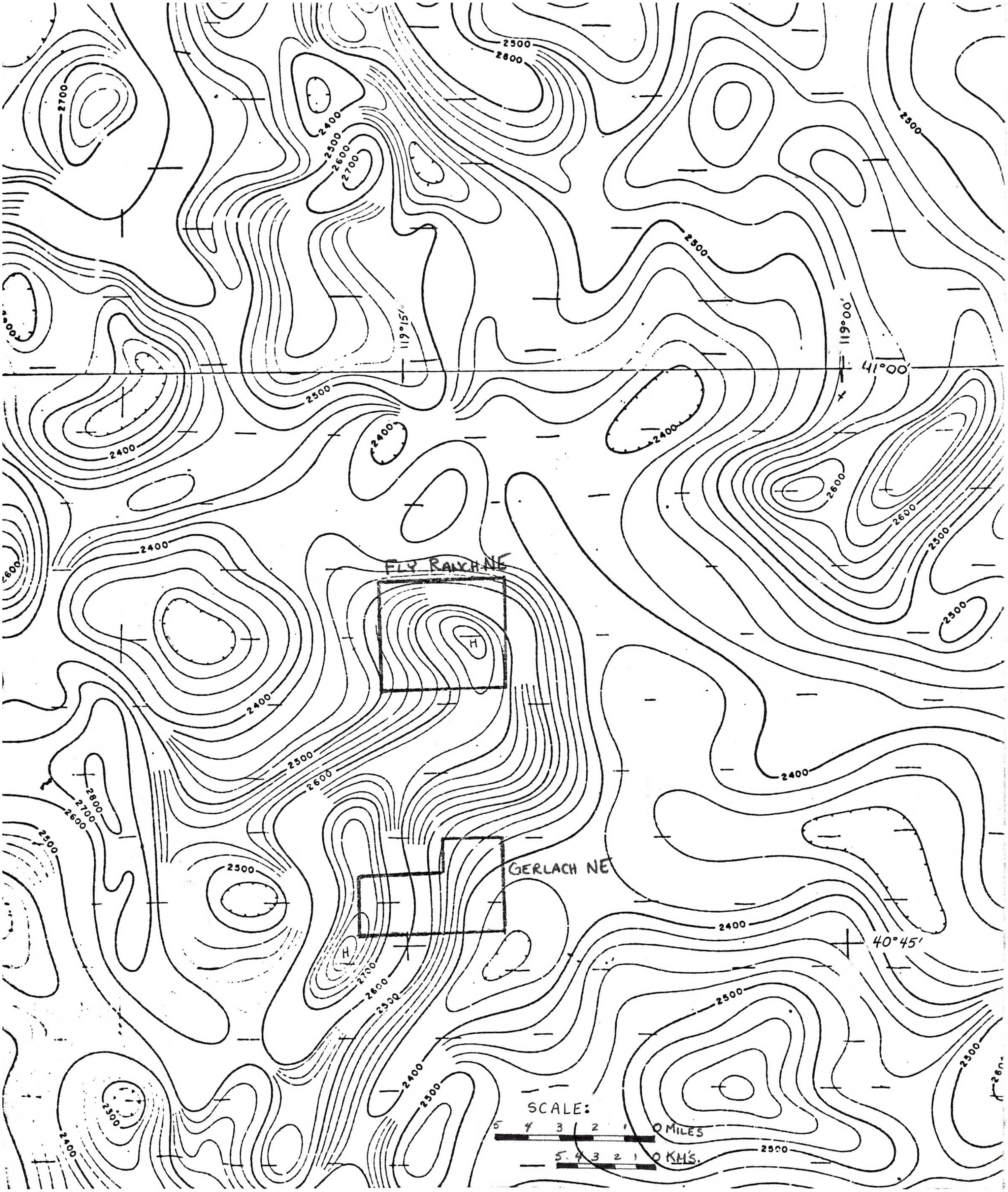

Fig. 4 Aeromagnetic Contour Map of the Fly Ranch NE and Gerlach NE KGRA's, Nevada

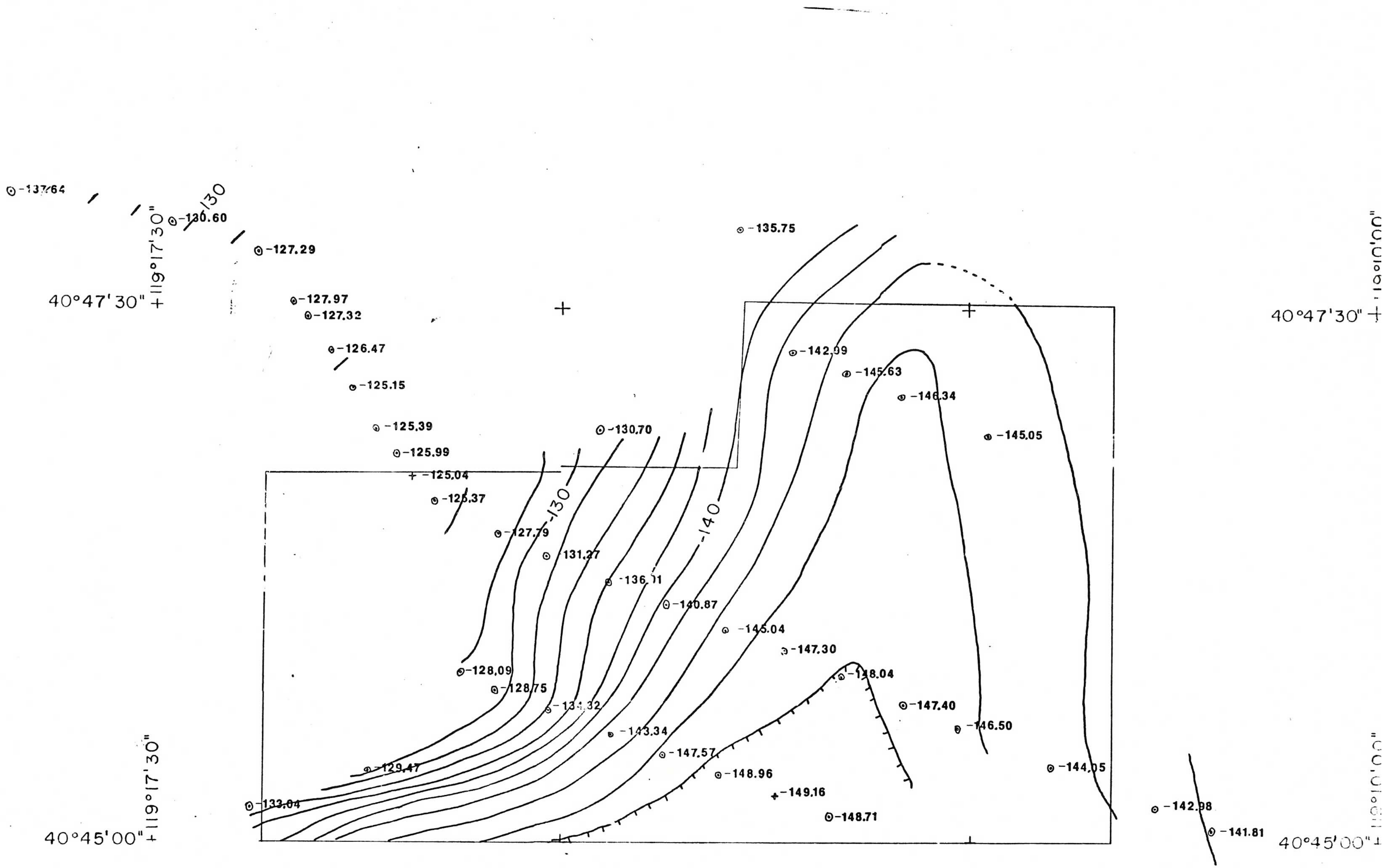

Fig. 5. Simple Bouguer Anomaly Map-Gerlach Northeast

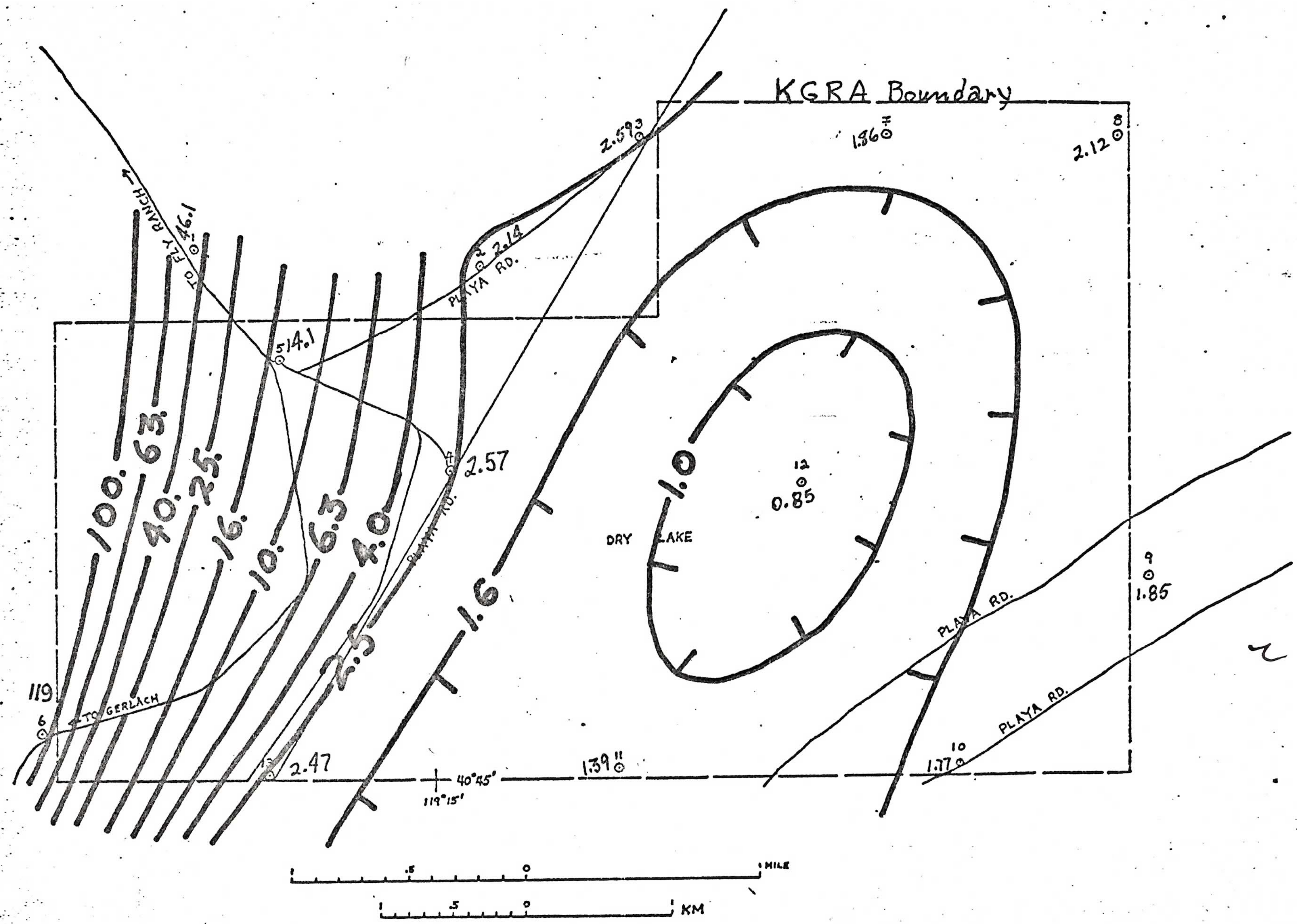

FIG. 6: AMT APPARENT RESISTIVITY MAP AT 7.5 hertz Avg.
GERLACH NE KGRA, NEVADA

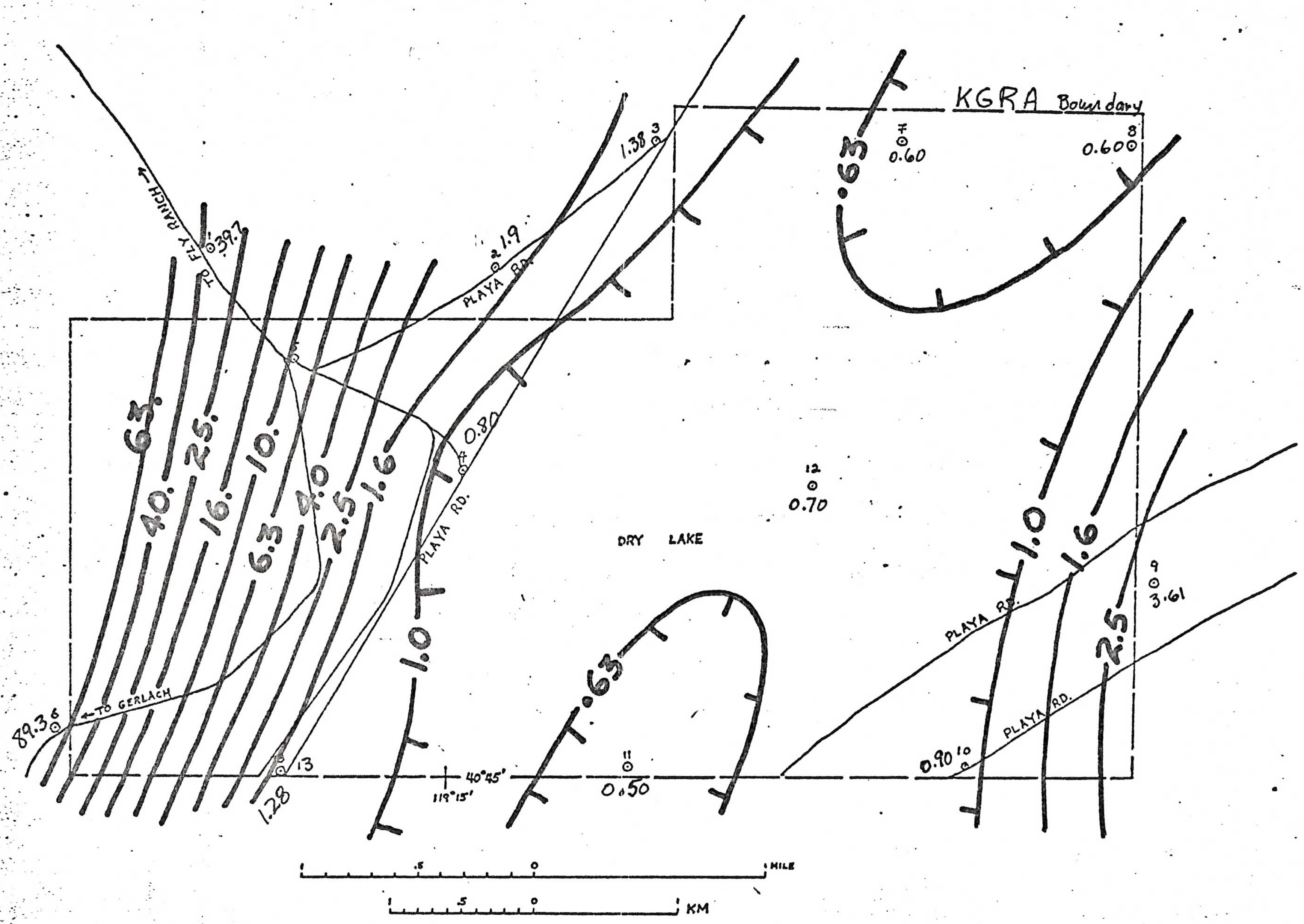

Fig: 7 AMT Apparent Resistivity Map at 27 hertz N-S
Gerlach NE KGRA, Nevada

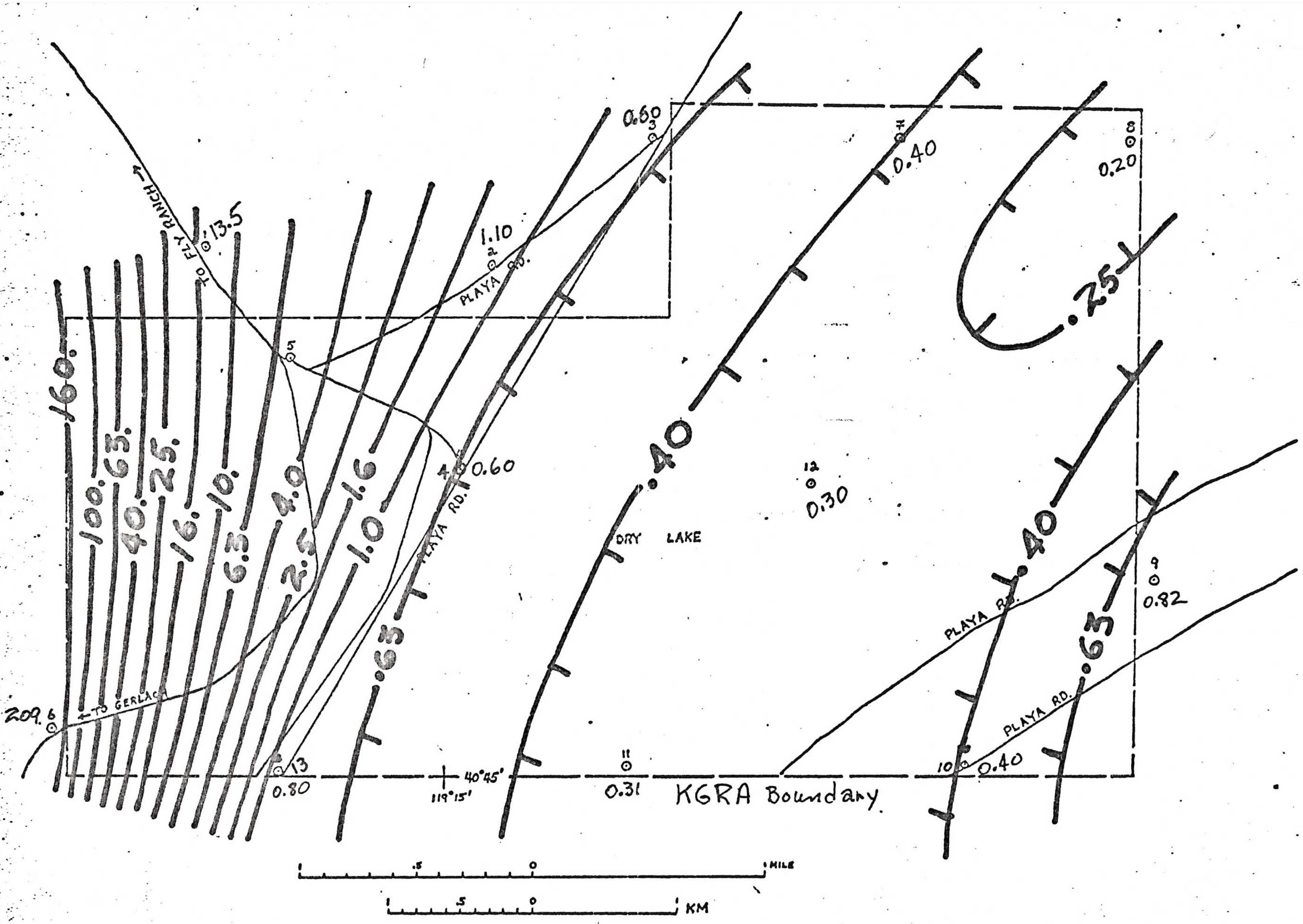

Fig. 8: AMT Apparent Resistivity Map at 27 hertz E-W
Gerlach NE KGRA, Nevada

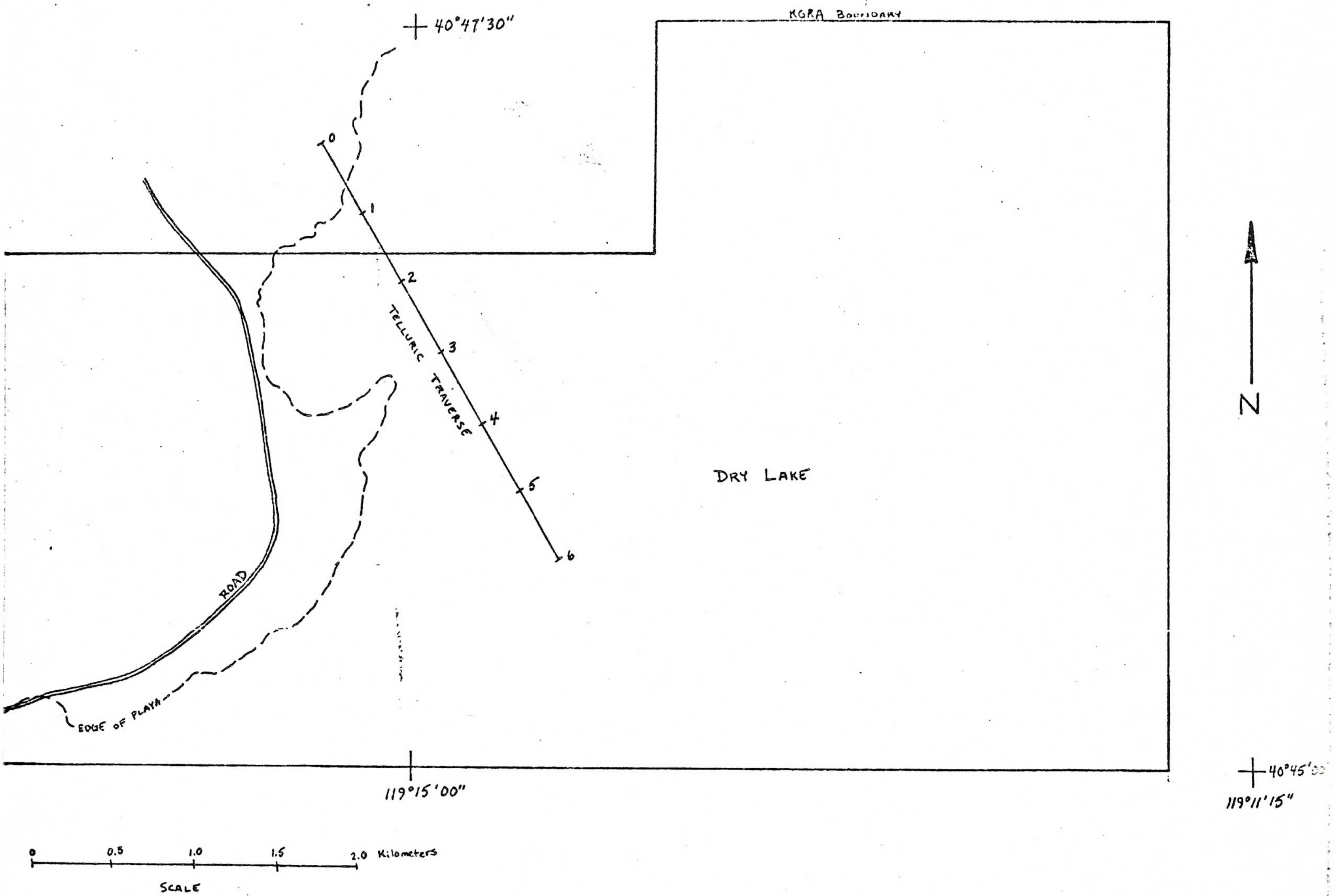

Fig. 9 Telluric Traverse Station Location Map
Gerlach Northeast KGRA - Nevada

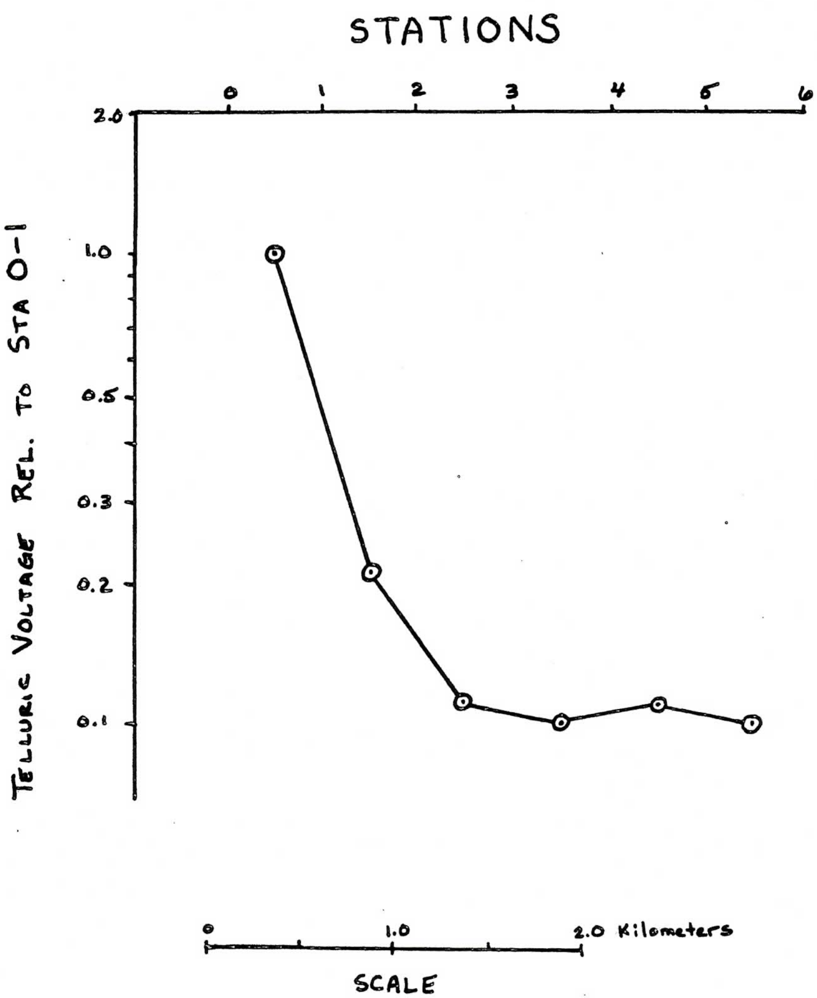

FIG. 10 TELLURIC PROFILE

GERLACH NORTHEAST KGRA
NEVADA

3.

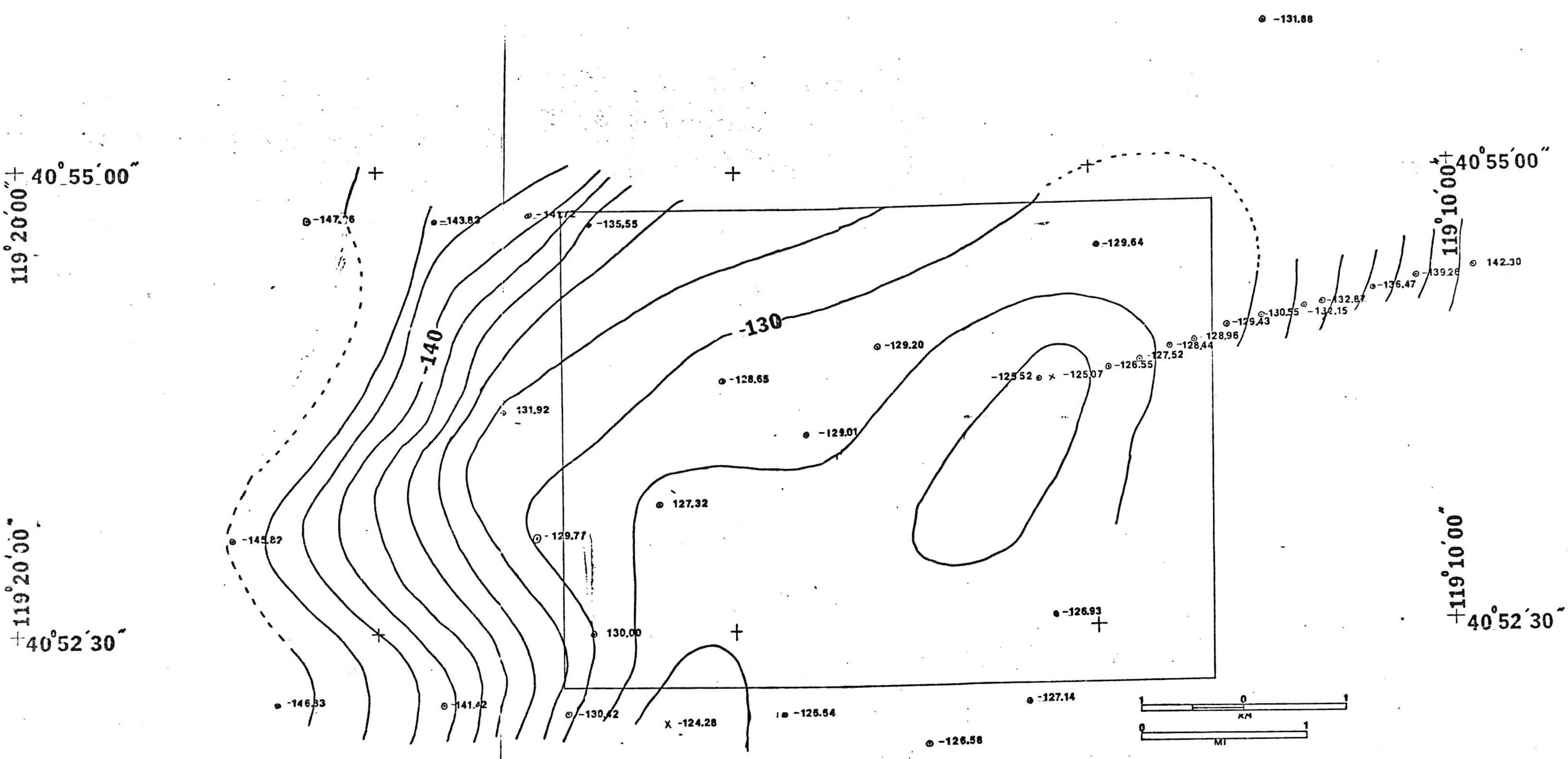

Fig. 11. Simple Bouguer Anomaly Map-Fly Ranch Northeast

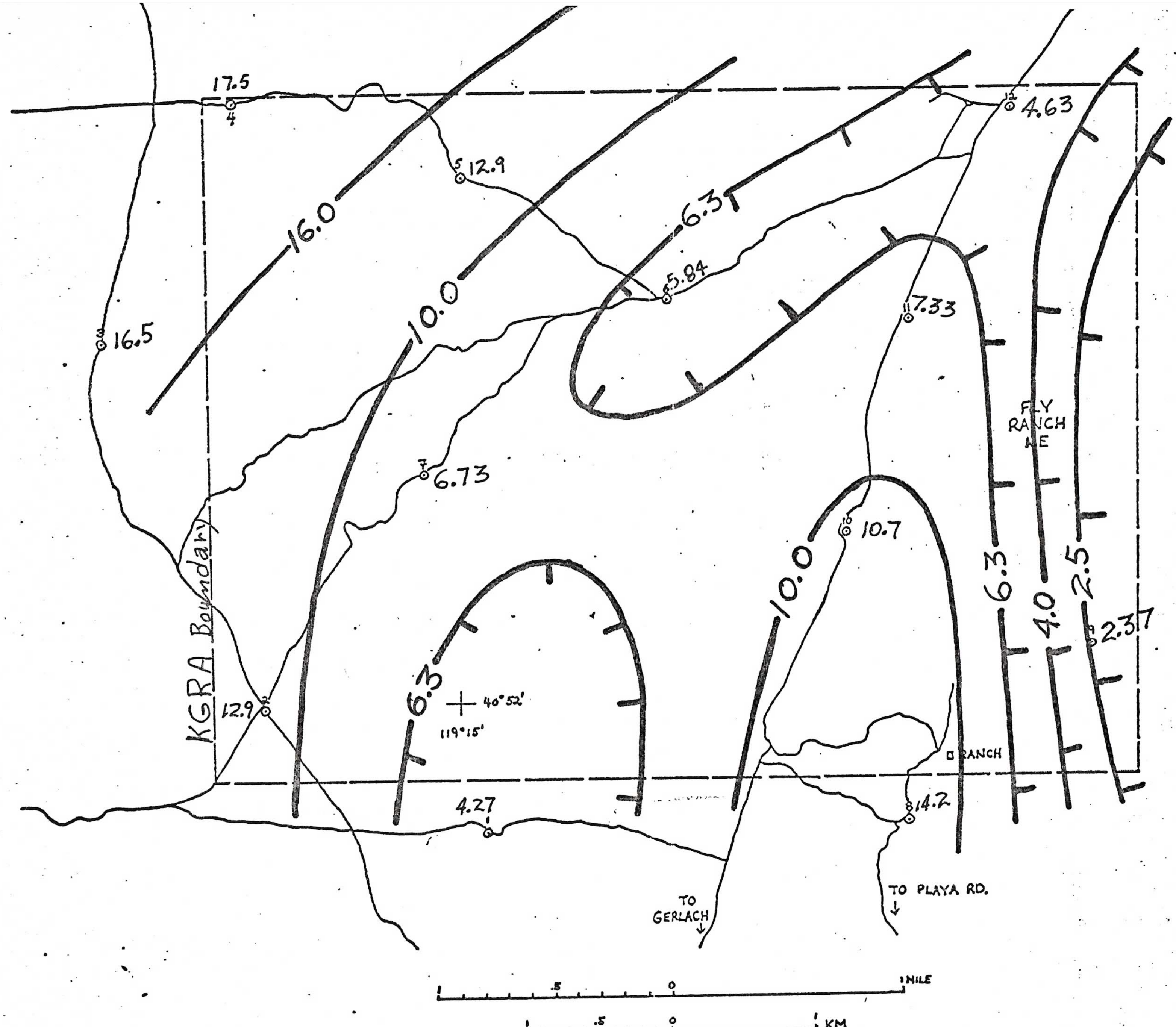

FIG 12: AMT APPARENT RESISTIVITY MAP AT 7.5 hertz Avg.
FLY RANCH NE KGRA, NEVADA

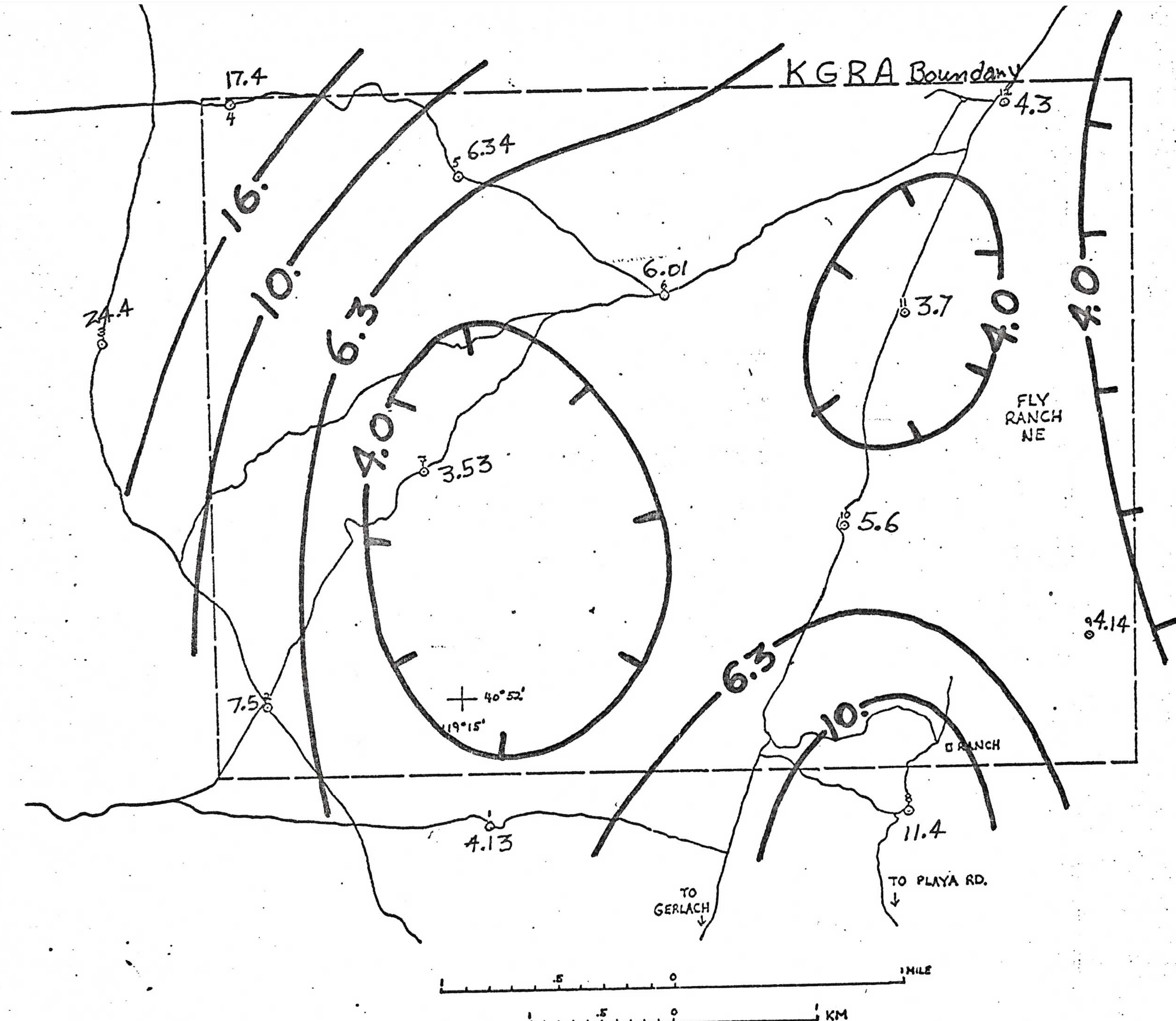

FIG 13: AMT APPARENT RESISTIVITY MAP AT 27 hertz N-S
FLY RANCH NE KGRA, NEVADA

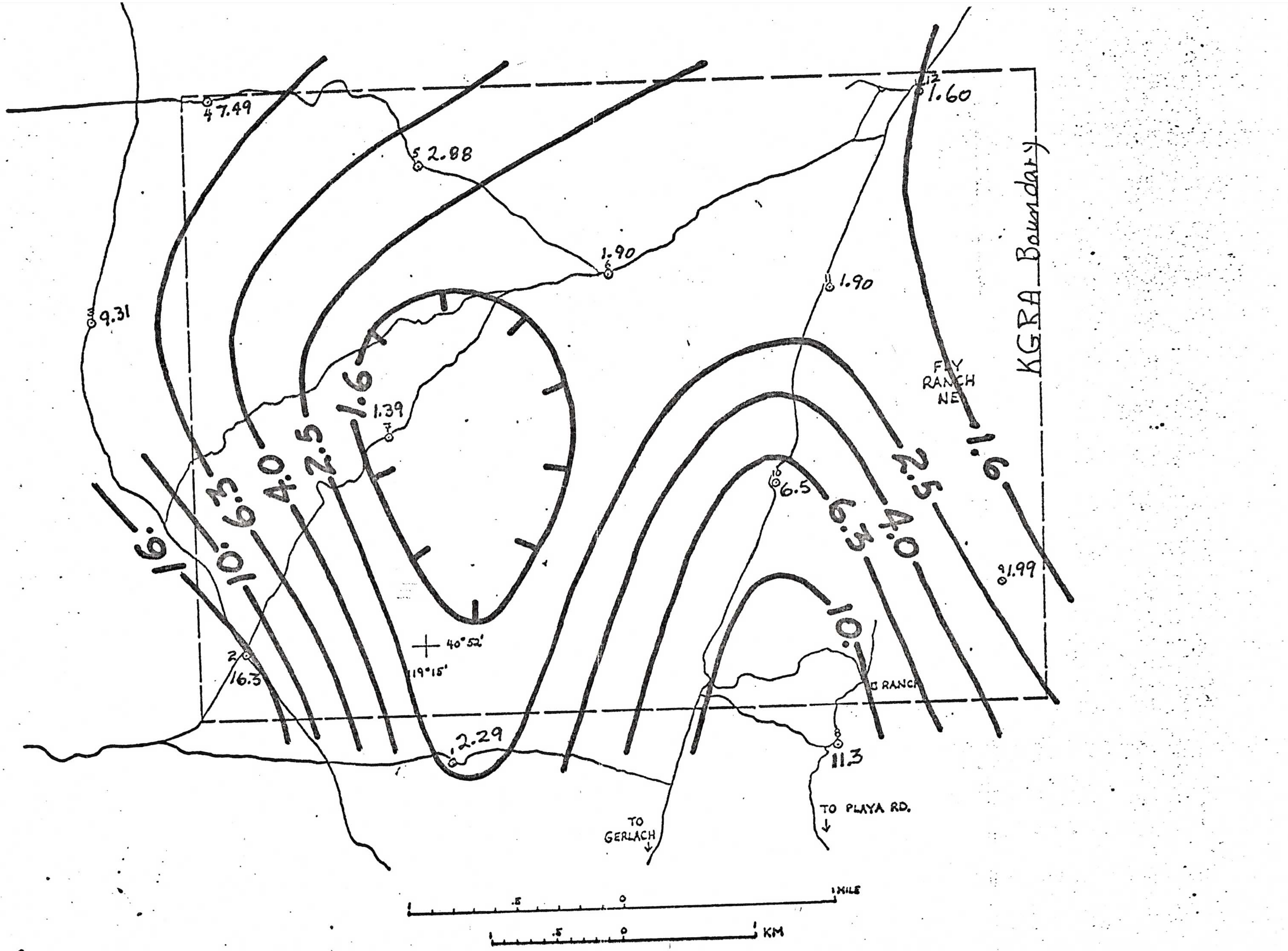

Fig 14: AMT Apparent Resistivity Map at 27 hertz E-W
Fly Ranch NE KGRA, Nevada

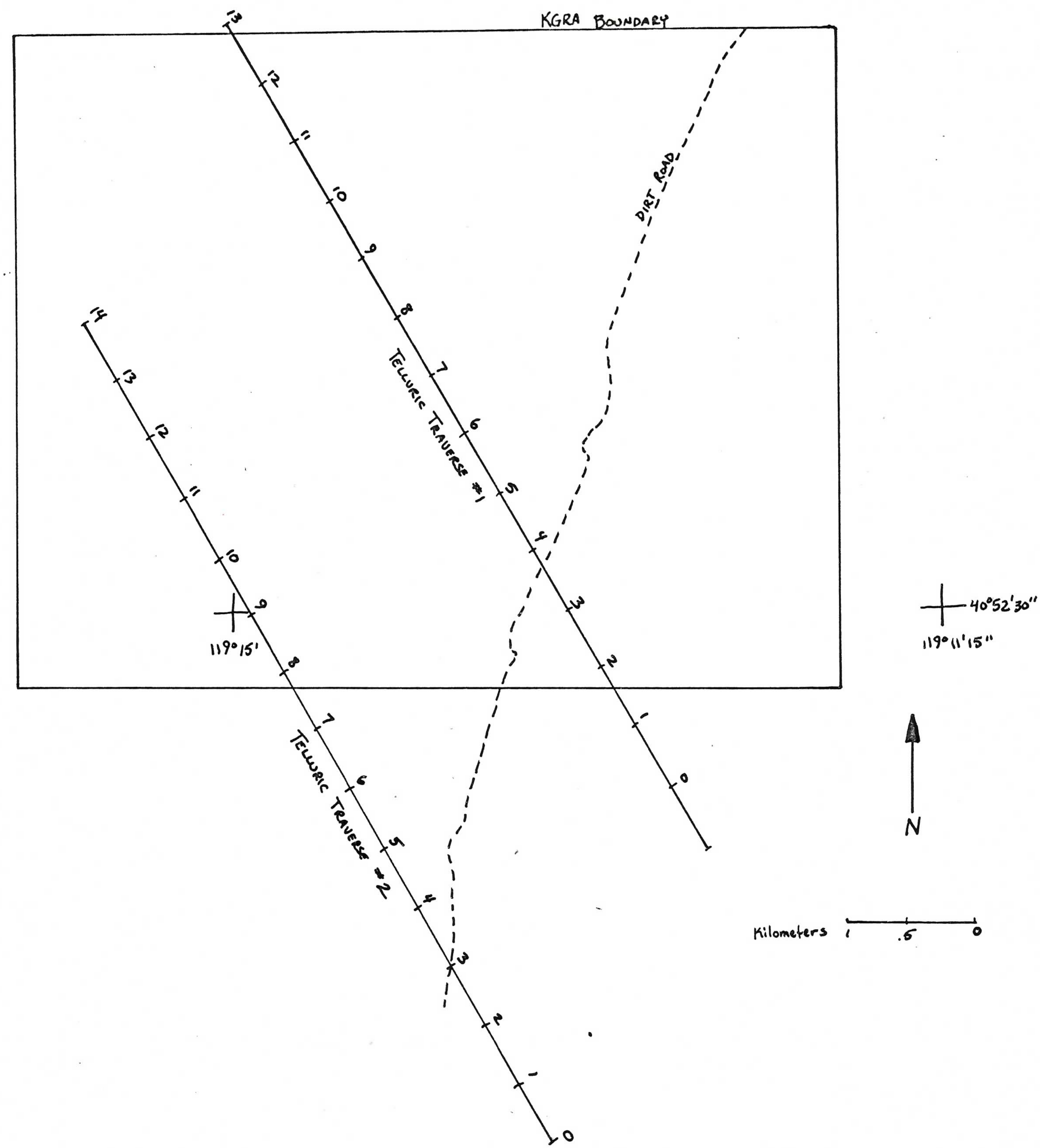

FIG 15 : TELLURIC TRAVERSE LOCATION MAP
FLY RANCH NE KGRA, NEVADA

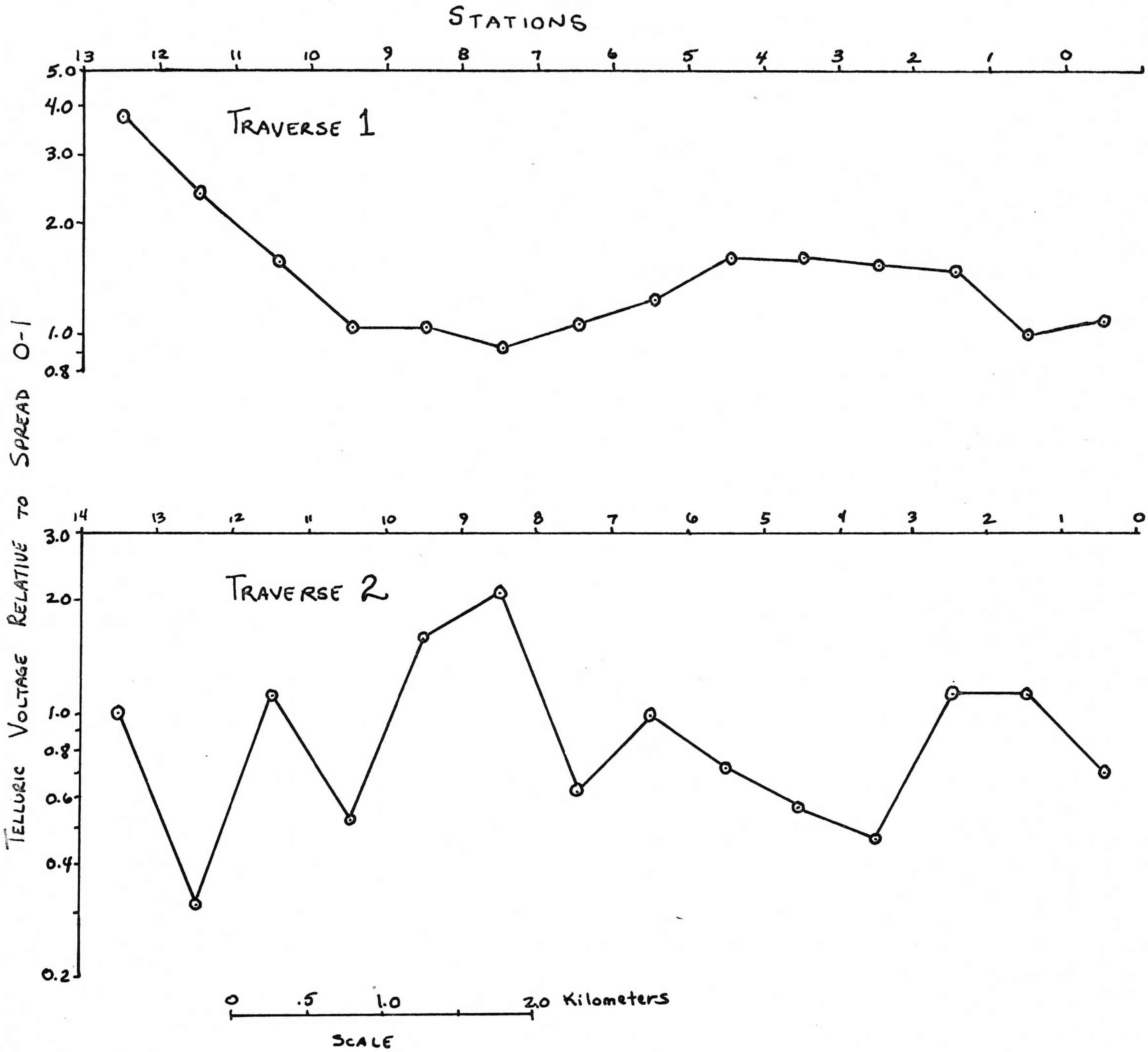

FIG 16: TELLURIC PROFILES - FLY RANCH NE KGRA, NEVADA

sta. no.	latitude	location longitude	elev,f	observed gravity	standard gravity	corrections fr.-air	corrections bouguer	anomalies fr.-air	anomalies bouguer
geex01	40 46.59	-119 15.77	3912.0	979879.73	-980238.28	367.85	-134.67	9.30	-125.37
geex02	40 46.70	-119 15.90	3934.0	979878.92	-980238.45	369.91	-135.42	10.38	-125.04
geex03	40 46.80	-119 16.01	3972.0	979875.85	-980238.60	373.49	-136.73	10.74	-125.99
geex04	40 46.92	-119 16.14	4011.0	979874.31	-980238.78	377.15	-138.07	12.68	-125.39
geex05	40 47.11	-119 16.29	4014.0	979874.65	-980239.06	377.43	-138.17	13.02	-125.15
geex06	40 47.30	-119 16.42	4057.0	979871.04	-980239.34	381.47	-139.64	13.17	-126.47
ex07	40 47.52	-119 16.65	4087.0	979868.07	-980239.67	384.30	-140.67	12.70	-127.97
geex08	40 47.45	-119 16.56	4083.0	979868.86	-980239.57	383.92	-140.53	13.21	-127.32
geex09	40 46.43	-119 15.37	3905.0	979877.50	-980238.05	367.19	-134.43	6.64	-127.79
geex10	40 46.33	-119 15.08	3905.0	979873.87	-980237.90	367.19	-134.43	3.16	-131.27
geex11	40 46.20	-119 14.70	3905.0	979868.93	-980237.70	367.19	-134.43	-1.58	-136.01
geex12	40 46.10	-119 14.34	3905.0	979863.92	-980237.55	367.19	-134.43	-6.44	-140.87
geex13	40 45.98	-119 13.99	3905.0	979859.58	-980237.38	367.19	-134.43	-10.61	-145.04
geex14	40 45.88	-119 13.62	3905.0	979857.17	-980237.23	367.19	-134.43	-12.87	-147.30
geex15	40 45.77	-119 13.27	3905.0	979856.26	-980237.06	367.19	-134.43	-13.61	-148.04
geex16	40 45.64	-119 12.90	3905.0	979856.7[illegible]	-980236.87	367.19	-134.43	-12.97	-147.40
geex17	40 45.53	-119 12.57	3905.0	979857.44	-980236.70	367.19	-134.43	-12.07	-146.50
geex18	40 45.35	-119 11.99	3905.0	979859.63	-980236.44	367.19	-134.43	-9.62	-144.05
geex19	40 45.16	-119 11.36	3905.0	979860.41	-980236.15	367.19	-134.43	-8.55	-142.98
geex20	40 45.05	-119 11.01	3905.0	979861.42	-980235.99	367.19	-134.43	-7.38	-141.81
geex21	40 47.75	-119 16.88	4004.0	979874.05	-980240.01	376.49	-137.83	10.54	-127.29
geex22	40 47.89	-119 17.40	3968.0	979873.10	-980240.22	373.11	-136.59	5.99	-130.60
geex23	40 48.03	-119 18.40	3982.0	979865.44	-980240.43	374.42	-137.07	-0.57	-137.64
geex24	40 48.02	-119 19.44	3993.0	979860.71	-980240.42	375.46	-137.45	-4.25	-141.70
geex25	40 45.78	-119 15.60	3974.0	979872.12	-980237.08	373.67	-136.80	8.71	-128.09
geex26	40 45.33	-119 16.18	3948.0	979871.61	-980236.41	371.23	-135.90	6.43	-129.47
geex27	40 45.16	-119 16.90	3942.0	979868.15	-980236.15	370.66	-135.70	2.66	-133.04
geex28	40 44.26	-119 17.59	3978.0	979858.[illegible]7	-980234.81	374.05	-136.93	-1.89	-138.82
geex29	40 43.77	-119 18.32	3960.0	979856.88	-980234.08	372.36	-136.32	-4.84	-141.16
geex30	40 42.88	-119 20.28	3936.0	979845.31	-980232.75	370.10	-135.49	-17.34	-152.83
geex31	40 44.67	-119 10.09	3939.0	979861.22	-980235.42	370.38	-135.60	-3.82	-139.42
geex32	40 44.27	-119 10.60	3967.0	979862.16	-980234.83	373.01	-136.56	0.34	-136.22
geex33	40 43.09	-119 10.29	4100.0	979846.59	-980233.07	385.52	-141.12	-0.96	-142.08
geex34	40 42.40	-119 10.19	4162.0	979838.59	-980232.04	391.35	-143.24	-2.10	-145.34
geex35	40 39.99	-119 19.55	3907.0	979834.14	-980228.45	367.37	-134.50	-26.94	-161.44
geex36	40 41.03	-119 17.78	3906.0	979845.80	-980230.00	367.28	-134.46	-16.92	-151.38
geex37	40 45.70	-119 15.39	3907.0	979875.34	-980236.96	367.37	-134.50	5.75	-128.75
geex38	40 45.61	-119 15.06	3905.0	979869.74	-980236.82	367.19	-134.43	0.11	-134.32
geex39	40 45.50	-119 14.69	3905.0	979860.56	-980236.66	367.19	-134.43	-8.91	-143.34
geex40	40 45.41	-119 14.37	3905.0	979856.19	-980236.52	367.19	-134.43	-13.14	-147.57

sta. no.	latitude	location longitude	elev,f	observed gravity	standard gravity	corrections fr.-air	bouguer	anomalies fr.-air	bouguer
geex41	40 45.32	-119 14.03	3905.0	979854.67	-980236.39	367.19	-134.43	-14.53	-148.96
geex42	40 45.22	-119 13.68	3905.0	979854.32	-980236.24	367.19	-134.43	-14.73	-149.16
geex43	40 45.12	-119 13.35	3905.0	979854.62	-980236.09	367.19	-134.43	-14.28	-148.71
geex44	40 44.97	-119 12.78	3905.0	979855.87	-980235.87	367.19	-134.43	-12.81	-147.24
GEEX45	40 46.91	-119 14.77	3905.0	979875.31	-980238.76	367.18	-134.43	3.73	-130.70
GEEX46	40 47.43	-119 13.91	3905.0	979871.04	-980239.54	367.18	-134.43	-1.32	-135.75
GEEX47	40 47.30	-119 13.58	3905.0	979863.60	-980239.34	367.18	-134.43	-8.56	-142.99
GEEX48	40 47.20	-119 13.25	3905.0	979860.81	-980239.19	367.18	-134.43	-11.20	-145.63
GEEX49	40 47.08	-119 12.91	3905.0	979859.92	-980239.01	367.18	-134.43	-11.91	-146.34
GEEX50	40 46.90	-119 12.38	3905.0	979860.95	-980238.75	367.18	-134.43	-10.62	-145.05
GEEX51	40 49.64	-119 12.05	3905.0	979874.97	-980242.83	367.18	-134.43	-0.68	-135.11

sta. no.	latitude	location longitude	elev,f	observed gravity	standard gravity	corrections fr.-air	corrections bouguer	anomalies fr.-air	anomalies bouguer
FREX01	40 51.39	-119 12.49	3908.0	979885.36	-980245.44	367.47	-134.53	7.39	-127.14
FREX02	40 52.10	-119 12.99	3919.0	979885.77	-980246.50	368.50	-134.91	7.77	-127.14
FREX03	40 51.89	-119 13.70	3919.0	979886.02	-980246.19	368.50	-134.91	8.33	-126.58
FREX04	40 52.06	-119 14.69	3948.0	979884.47	-980246.44	371.23	-135.90	9.26	-126.64
FREX05	40 52.01	-119 15.48	3989.0	979884.32	-980246.37	375.08	-137.31	13.03	-124.28
FREX06	40 52.07	-119 16.17	3981.0	979878.75	-980246.46	374.33	-137.04	6.62	-130.42
FREX07	40 52.12	-119 17.04	3980.0	979867.88	-980246.53	374.23	-137.00	-4.42	-141.42
FREX08	40 52.13	-119 18.20	3985.0	979862.18	-980246.55	374.71	-137.17	-9.66	-146.83
FREX09	40 53.00	-119 18.49	4012.0	979862.89	-980247.65	377.24	-138.10	-7.72	-145.82
FREX10	40 53.00	-119 20.50	4059.0	979859.43	-980247.85	381.66	-139.71	-6.76	-146.47
FREX11	40 54.73	-119 19.67	4071.0	979854.25	-980250.43	382.79	-140.12	-13.39	-153.51
FREX12	40 54.73	-119 17.96	4039.0	979862.62	-980250.43	379.78	-139.03	-8.03	-147.06
FREX13	40 54.74	-119 17.09	4027.0	979866.57	-980250.44	378.65	-138.61	-5.22	-143.83
FREX14	40 54.77	-119 16.43	4032.0	979868.44	-980250.49	379.12	-138.79	-2.93	-141.72
FREX15	40 54.71	-119 16.01	4112.0	979869.74	-980250.40	386.64	-141.53	5.98	-135.55
FREX16	40 54.94	-119 45.25	4351.0	979860.02	-980250.74	409.11	-149.72	18.39	-131.33
FREX17	40 52.56	-119 12.79	3929.0	979886.07	-980247.19	369.44	-135.25	8.32	-126.93
FREX18	40 53.83	-119 12.86	3942.0	979888.60	-980249.08	370.66	-135.70	10.18	-125.52
FREX19	40 54.57	-119 12.46	3959.0	979884.57	-980250.19	372.26	-136.28	6.64	-129.64
FREX20	40 55.78	-119 11.24	3969.0	979883.54	-980251.99	373.20	-136.63	4.75	-131.88
FREX21	40 54.03	-119 13.99	3970.0	979883.54	-980249.38	373.30	-136.66	7.46	-129.20
FREX22	40 53.97	-119 14.51	3975.0	979883.34	-980249.29	373.77	-136.83	7.82	-129.01
FREX24	40 52.49	-119 15.98	3979.0	979879.91	-980247.08	374.14	-136.97	6.97	-130.00
FREX25	40 53.02	-119 16.37	3995.0	979879.98	-980247.88	375.65	-137.52	7.75	-129.77
FREX26	40 53.70	-119 16.62	4065.0	979874.67	-980248.89	382.22	-139.92	8.00	-131.92
FREX27	40 53.19	-119 15.52	3983.0	979883.40	-980248.13	374.52	-137.11	9.79	-127.32
FREX28	40 53.65	-119 15.09	3992.0	979882.51	-980249.11	375.36	-137.41	8.76	-128.65
FREX29	40 54.51	-119 8.82	3905.0	979865.52	-980250.10	367.18	-134.43	-17.40	-151.83
FREX30	40 54.48	-119 9.15	3905.0	979869.30	-980250.05	367.18	-134.43	-13.57	-148.00
FREX31	40 54.44	-119 9.48	3905.0	979872.35	-980249.99	367.18	-134.43	-10.46	-144.89
FREX32	40 54.41	-119 9.82	3905.0	979874.90	-980249.95	367.18	-134.43	-7.87	-142.30
FREX33	40 54.36	-119 10.22	3905.0	979877.87	-980249.88	367.18	-134.43	-4.83	-139.26
FREX34	40 54.30	-119 10.52	3905.0	979880.57	-980249.79	367.18	-134.43	-2.04	-136.47
FREX35	40 54.23	-119 10.88	3905.0	979884.06	-980249.68	367.18	-134.43	1.56	-132.87
FREX36	40 54.21	-119 11.00	3905.0	979884.75	-980249.65	367.18	-134.43	2.28	-132.15
FREX37	40 54.16	-119 11.31	3922.0	979885.26	-980249.58	368.78	-135.01	4.46	-130.55
FREX38	40 54.11	-119 11.54	3923.0	979886.24	-980249.50	368.88	-135.05	5.62	-129.43
FREX39	40 54.03	-119 11.77	3926.0	979886.46	-980249.38	369.16	-135.15	6.24	-128.91
FREX40	40 54.00	-119 11.94	3929.0	979886.71	-980249.34	369.44	-135.25	6.81	-128.44
FREX41	40 53.93	-119 12.15	3931.0	979887.40	-980249.23	369.63	-135.32	7.80	-127.52

sta. no.	latitude	location longitude	elev, f	observed gravity	standard gravity	corrections fr.-air	corrections bouguer	anomalies fr.-air	anomalies bouguer
FREX42	40 53.90	-119 12.38	3933.0	979888.21	-980249.19	369.82	-135.39	8.84	-126.55
FREX43	40 53.85	-119 12.78	3939.0	979889.26	-980249.11	370.38	-135.60	10.53	-125.07
FREX44	40 56.22	-119 7.95	3905.0	979866.60	-980252.65	367.18	-134.43	-18.87	-153.30